Climatology and changes in cloud cover in the area of the Black, Caspian, and Aral seas (1991-2010): a comparison of surface observations with satellite and reanalysis products

Josep Calbó (1), Jordi Badosa (2), Josep-Abel González (1), Lidya Dmitrieva (3), Valentina Khan (3), Aaron Enríquez-Alonso (1), Arturo Sanchez-Lorenzo (1,4)

(1) Environmental Physics Group, Department of Physics, Universitat de Girona, Girona, Spain
(2) Laboratoire de Météorologie Dynamique (LMD), Ecole Polytechnique, Palaiseau, France
(3) Hydrometeorological Research Center of the Russian Federation, Moscow, Russia
(4) Instituto Pirenaico de Ecología, Consejo Superior de Investigaciones Científicas (IPE-CSIC), Zaragoza, Spain

Corresponding author: Josep Calbó, josep.calbo@udg.edu

Abstract

The present paper presents a climatology of total cloud cover (TCC) in the area of the three inland Eurasian seas (Black, Caspian, and Aral Sea). Analyses are performed on the basis of 20 years of data (1991-2010), collected from almost 200 ground stations. Average TCC is 49%, with broad spatial and seasonal variability: minimum TCC values are found in summer and to the southeast, while maximum values correspond to winter and to the northwest. For the whole area, linear trend analyses show that TCC did not vary during the study period. We only detected a statistically significant positive trend (+1.2% decade^{-1}) in autumn. We obtained different results for the regions delimited by means of a Principal Component Analysis: a clear decrease, both for the annual, spring, and summer series, was detected for the south of Black Sea, while increasing TCC was found for the annual, autumn, and winter series in the north Caucasus and the west and north of Black Sea. We also analyzed the TCC data from global gridded products, including satellite projects (ISCCP, PATMOS-x, CLARA), reanalyses (ERA-interim, NCEP/DOE, MERRA), and surface observations (CRU). Although all these products capture the seasonal evolution over the study area, they differ substantially both among them and in relation to the ground observations: reanalyses produce much lower values of TCC, while ISCCP and CLARA provide a summer minimum that is too high. Trend analyses applied to these data generally showed a decrease in TCC; only CRU and NCEP/DOE tally with the ground data as regards the absence of overall trends. These results are discussed in relation to previous studies presenting trends of other variables such as sunshine duration, diurnal temperature range or precipitation; we also discuss the connections with changes in synoptic patterns and environmental changes, in particular in the Aral Sea region.

Key words: total cloud cover, climatology, variability, trends, Black Sea, Caspian Sea, Aral Sea

1. Introduction

Clouds play a key role in the Earth's energy balance and hydrological cycle, both at global and local scales (Ramanathan *et al*., 1989; Stevens and Bony, 2013). The physical mechanism of the influence of clouds on the underlying surface involves the way they affect the heat balance, which determines surface temperature (Matuszko and Węglarczyk, 2014). For example, a numerical experiment performed using the mesoscale hydrodynamical model COSMO for the European part of Russia showed that variations in the radiative fluxes between cloudless and cloudy situations may be as great as hundreds of Wm^{-2} (Yevteev *et al*., 2010).

Within the framework of current climate change, the recent report by the Intergovernmental Panel on Climate Change emphasized the uncertainties associated with clouds in relation to past climate, particularly regarding model simulations of future climate (Nam *et al*., 2012; Boucher *et al*., 2013). Despite the advances made in the modeling of the climate system, little progress has been made with regard to describing cloud-related physical processes in the models. Phenomena such as cloud formation, dissipation, precipitation, and effects on radiative fluxes are usually parameterized on the resolved scales. It is well known that many processes in climate systems are governed by cloud feedbacks through radiative and latent heat fluxes in the atmosphere. Uncertainties in the simulation of clouds therefore provide a wide range of climate model results and may lead to noteworthy regional errors relating to cloud radiative effect (Flato *et al*., 2013).

Climatic studies of cloudiness are by far less common than studies concerning other variables such as temperature or precipitation. This is in part due to the difficulty involved in obtaining reliable data on clouds: prior to the satellite era, the only way to obtain cloud data was through visual observation by experienced meteorological personnel (Sanchez-Lorenzo *et al*., 2012). These observations were therefore limited to manned stations, so their spatial (and temporal) density is lower than other meteorological variables. An additional issue refers to the intrinsic subjectivity allocated to these observations, in particular when distinguishing scattered or broken clouds and classifying the cloud type. An example of this kind of problems involves the U.S cloud cover database, for which Free and Sun (2013, 2014) remark the need for testing and adjustment before it can be used with confidence for climate trend assessment or satellite product validation. This is due to the disruption of such observations by the introduction of automated observation systems and other artificial shifts.

As from the last three decades, satellite imagery can offer a more complete view of cloudiness, although several remarkable issues regarding the spatial/temporal resolution and long-term homogeneity of these data have been identified (Norris, 2005; Evan *et al*., 2007; Cermak *et al.*, 2010; Sun *et al*., 2015). Indeed, the satellite view is complementary, but by nature different from classical ground-based observations, in terms of point of view and of spatial and temporal resolutions (e.g. L'Ecuyer and Jiang, 2010). Recently, sky cameras and other (active) devices such as ceilometers or cloud radars are being deployed to further characterize cloud behavior from the ground (Long *et al*., 2006; Costa-Surós *et al*., 2013; Klebe *et al*., 2014); radiosoundings can also be used to describe cloud structure (Costa-Surós *et al*., 2014).

Despite the above mentioned issues, there have been publications providing several climatic descriptions of cloud behavior within both the global and regional scopes. For example, Warren *et al*. (2007) developed a global climatology of clouds based upon the so-called Extended Edited Cloud Report Archive (EECRA) dataset, which contains synoptic observations for oceans since 1952 and for continents since 1971; moreover, they studied the long-term changes. The aforementioned dataset has been updated and a more indepth analysis is given in Eastman and Warren (2013). Other studies are also of interest: at continental scale we can mention the works of Henderson-Sellers (1992) for Europe, Dai *et al*. (2006) and Free and Sun (2014) for the USA, Kaiser (2000) and Xia (2012) for China, and Sun and Groisman (2000) for the former Soviet Union (FUSSR) or Chernokulsky *et al*. (2011) for Russia. At a more local scale, Calbó and Sanchez-Lorenzo (2009) studied the cloud climatology of the Iberian Peninsula. Further information on cloud climatology studies can be found in Warren and Hahn (2002) and a review of studies on long-term evolutions of cloudiness is presented by Sanchez-Lorenzo *et al.* (2012).

The present study focuses on changes in cloudiness (specifically total cloud cover, TCC), over the last 20 years, in and around the Eurasian inland seas: the Black Sea, the Caspian Sea and the Aral Sea. This area is the object of CLIMSEAS (Climate Change and Inland Seas: Phenomena, Feedbacks, and Uncertainties. The Physical Science Basis), a recent European project that involved researchers from Russia, Spain, the United Kingdom, and the United States. The belt of middle latitudes encompassing the Black, Caspian, and Aral seas area is of particular interest due to its geographical position, the presence of the three inland seas (which may affect climate at regional scales), and the recent environmental changes resulting from strong anthropogenic pressures, namely the shrinking of the Aral Sea (Koronkevich and Zaitseva, 2003; Shiklomanov and Vasilieva, 2003; Chub, 2007; Aus der Beek *et al*., 2011; Gaybullaev *et al.*, 2012; Zavialov *et al*., 2012; Frolov, 2014; Rubinstein *et al*., 2014).

The components of the water and the heat budgets of these enclosed and inland seas are particularly dependent on local meteorological and hydrological conditions and are therefore highly sensitive to climate change (Shiklomanov and Vasilieva, 2003; Chub, 2007; Zavialov *et al*., 2012; Frolov, 2014; Rubinstein *et al*., 2014). Hence, information on the temporal changes in the climate variables of the study area and their spatial patterns is important. It can provide insights into the complex mechanism of interactions and mutual feedbacks between local atmospheric circulation, heat fluxes, and the components of hydrological cycles of the seas.

Much is now known of the ecological disaster involving the desiccation of the Aral Sea, which resulted both from anthropogenic pressure and from the impact of climate change (e.g. Khan *et al*., 2004; Roget *et al*., 2009; Zavialov *et al*., 2012). A variety of scientific and practical issues exist referring to level changes in the Caspian Sea that are modulated by regional climate variability (e.g. Meshcerskaya and Golod, 2003; Arpe *et al*. 2012, 2014). More recent publications (e.g. IPCC 2014; Frolov, 2014) highlighted the vulnerability and sensitivity of the Black Sea ecosystems in relation to climate-mediated hypoxia, eutrophication, and pollution. The key question to be addressed involves the extent to which human activity could have altered the physical, chemical and biological characteristics of the seas, and how these changes impacted the local climate.

Regarding time variations in cloudiness, Sun and Groisman (2000) found an overall increase in TCC in the FUSSR for the 1945-1990 period, on analyzing data from surface stations. For the western part of the FUSSR (where our study area is located), the increase was statistically significant in summer (0.7 %TCC decade^{-1}, where %TCC means fraction of sky covered by clouds). A study by Tang and Leng (2012) used daytime satellite-derived TCC data from PATMOS-x, confirming the general TCC increase over most areas of Eurasia in the 1982-2009 period. This latter paper, however, shows that the increase in TCC is not as evident in our study area; specifically, for the 1995-2009 subperiod, a decrease in TCC (from -2 to over -6 %TCC decade^{-1}) affects the northern regions of the area. A more detailed study of clouds based upon visual observations at Russian meteorological stations over a 20-year (1991-2010) period (Chernokulsky *et al*., 2011) shows that in the north of the Caucasus, between the Black and the Caspian Sea, daytime TCC tends to increase, particularly in autumn and winter (approximately 1 %TCC decade^{-1}), and much less remarkably in summer and spring.

The present paper aims at presenting the climatology of TCC in the area of the inland Eurasian seas, providing both the mean annual and seasonal values and also the interannual variability and trends during the last two decades, based upon observations from almost 200 ground meteorological stations in the area. In addition, several global gridded products (satellite, reanalysis, and surface data) are also used for further study of TCC in the area.

2. Data

2.1 Ground-based raw data

The basic data for the present study was provided by the Hydrometeorological Center of the Russian Federation (RHMC) and consists of standard synoptic observations taken at hundreds of stations in the area of interest (35-52ºN, 25-70ºE; see Figure 1). The stations currently belong to fourteen countries: Russia, Ukraine, Moldova, Romania, Bulgaria, Turkey, Greece, Georgia, Armenia, Azerbaijan, Iran, Turkmenistan, Uzbekistan, and Kazakhstan. The dataset covers the January 1991- July 2010 period.

For each station, the corresponding files contain measurements and observations of most meteorological variables. In relation to cloudiness, all files provide observations of TCC; depending on station and period, data are also available on cloud type or the height of the lowest cloud. Due to the discontinuities and diversity of the latter observations, the present study will only focus on TCC. This variable is provided both for daytime and nighttime, every 3 or 6 h, depending also on station/period. In order to avoid bias resulting from the different observation times, we finally only employed the four observations per day (at 00, 06, 12, 18 h UTC, i.e., covering the whole daily cycle) that were available for all stations and periods. The method used to register the TCC was changed during the study period: from 1991 to 2002, TCC was in oktas, whereas after 2005, TCC is in tenths; during the 2003-04 period, some stations avail of a mixture of records in oktas and tenths, and close inspection of data for these years was therefore performed. Actually, we found that this simply involved a change in recording criteria: observations were actually performed in oktas as previously, but then recorded on a scale from 0-10, by means of direct conversion (oktas-tenths: 0-0, 1-1, 2-2, 3-4, 4-5, 5-6, 6-7, 7-9, 8-10) which does not exactly follow the WMO recommendations (WMO, 2012). All TCC ground observations were converted into oktas for this study. That is, as from 2003, when some cloud observations were recorded in “tenths”, we changed the units back to oktas, in order to provide coherent series for the whole period analyzed. The estimated uncertainty associated with these changes is less than 0.1 oktas (1.25 %TCC) for the monthly means of TCC.

An equivalent dataset compiled by Hahn, Warren and Eastman (hereafter HWE, see Hahn and Warren, 2003; Eastman and Warren, 2013) was also available for our study and initially covers the 1971-2009 period. This dataset was not used due to the lack of available data for our main period of interest (1991-2009). Indeed, after application of our strict quality control procedure (see Section 3), the number of stations passing the tests (185) was about three times higher with our database than with the HWE dataset; in addition, the former presented more uniform spatial coverage of our region of interest than the latter (for example, many series of the former Soviet Union countries are not fully updated after 1997 in HWE). Moreover, the overall results obtained from both datasets are very similar (not shown), which supported our choice. Nevertheless, the HWE dataset may be very useful for extensive analyses similar to those presented in our paper, if applied to other regions and/or when focusing on the longer period starting in the 1970s.

2.2 Other datasets

Apart from the observations taken at meteorological stations, there exists a number of global datasets providing information about clouds on a regular grid. A selection of these datasets was considered in the present study, initially with the aim of complementing the results obtained by means of the raw observations, thus giving a more complete picture of the TCC climatology (You *et al.*, 2014). A side (yet relevant) result of the use of these datasets involves an assessment of their usefulness and shortcomings in relation to TCC in the area.

Three types of data were selected: satellite-derived data, reanalysis, and gridded data from ground observations. The specific products/datasets are detailed as following:

- The International Satellite Cloud Climatology Project (ISCCP) is a project of the World Climate Research Programme (WCRP), which attempts to study the role played by clouds in the Earth's radiation balance with the use of radiances measured from polar and geo-stationary satellites. Data were collected and processed from July 1983 to 2009 (Rossow and Schiffer, 1999; Rossow and Dueñas, 2004). In the present study we consider the TCC monthly mean values (produced from initial data at a temporal resolution of 3 hours) provided in the D2 dataset on an equal-area grid (280×280 km^2).

- PATMOS-x (Pathfinder Atmospheres Extended) provides data corresponding to different variables, including TCC, since 1981 (Foster and Heidinger, 2013). Variables are retrieved from the two daily fields produced by the Advanced Very High Resolution Radiometer (AVHRR) sensors onboard the Polar-orbiting Operational Environmental satellites (POES constellation) operated by NOAA, and more recently onboard the MetOp satellites operated by EUMETSAT. The resolution of the PATMOS-x data as downloaded and used in the present research is 1º×1º. Four observations per day (at 1:30, 7:30 am and 1:30, 7:30 pm) were used to compute daily, and subsequently monthly, averages, except in 1991, when only the morning and evening observations were available.
- The CM SAF cLoud, Albedo & Radiation dataset (CLARA), developed by the EUMETSAT Satellite Application Facility on Climate Monitoring (CM SAF) project, has a resolution of 0.25º × 0.25º and currently covers the period ranging from 1982 to 2009 (Karlsson *et al.*, 2013). It consists of TCC and other variables derived from the AVHRR sensors on the same satellite constellation as the PATMOS-x products, although TCC values are produced by different algorithms. In this case, the monthly averages as provided by EUMETSAT were used.
- ERA-Interim is the new generation of reanalysis provided by the ECMWF (European Centre for Medium-Range Weather Forecasts). ERA-Interim has a resolution of 0.75º × 0.75º and covers from 1979 until the present at a temporal resolution of 6 hours (Dee *et al.*, 2011), although the monthly means as provided by ECMWF were used in our study.
- The National Centers for Environmental Prediction / Department of Energy (NCEP/DOE) Atmospheric Model Intercomparison Project (AMIP-II) Reanalysis 2 (R-2) project provides data since 1979 every 6 hours at a spatial resolution of

approximately 1.9° × 1.9°; it uses an analysis/forecast system to perform assimilation of past data (Kanamitsu *et al.* 2002). Again, the monthly means were directly taken from the developers of this dataset.

- MERRA stands for Modern-Era Retrospective Analysis for Research and Applications and is intended to constitute a climate-quality analysis that places NASA's satellite observations within a climate context. MERRA data are available since 1979 on a 1/2˚ latitude × 2/3˚ longitude grid. As with the other products, the monthly means were used in the present study, despite the fact that data at 1-hour intervals are available (Rienecker *et al.*, 2011).
- The Climatic Research Unit (CRU) TS (time-series) gridded products provide monthly data for different meteorological variables, TCC being one of these. The datasets are based on an archive of thousands of meteorological stations throughout the world during the 1901-2011 period, and are transformed on a grid of 0.5º × 0.5º over land areas (Harris *et al.*, 2014). CRU cloudiness data are based only on day-time observations.

It should be noted that all these datasets offer a product that is labeled as TCC (or an equivalent term), which does not mean that the definition of clouds is exactly the same for all of them, and moreover, satellites view clouds from a different point of view. In addition, the different time resolutions of the original data may affect the comparison to a certain extent, although the latter issue should be minimized when working with monthly averages. The fact that the study region extends across several time zones could lead to slight differences in the way the daily cycle is captured in each region.

3. Methods: quality control, regionalization, trend analysis

Initially, data files corresponding to several hundreds of stations in the area were available for this research. Several quality control criteria were imposed upon each station in order for them to be included in the final database. First, we aggregated the four values of TCC per day into monthly mean TCC, by simply performing an arithmetic averaging. Months with over 50% of missing original TCC data were labeled as “no data”. We then discarded all stations with over 20% of missing months. Subsequently, a quality control based upon visual inspection of all monthly series was also applied and some stations presenting obvious temporal inhomogeneity were removed from the database.

Like most meteorological variables, TCC exhibits a strong yearly cycle; in order to remove this from some analyses (trends, regionalization), we computed monthly TCC anomalies. Anomalies are defined as the difference between the actual monthly value and the mean value for that month during the whole series (1991-2009 period):

$$TCC_{anom}(j,k) = TCC(j,k) - \frac{\sum_{m=1}^{Nj} TCC(j,m)}{Nj} \qquad (1)$$

where $TCC(j,k)$ is the TCC for month j of year k, TCC_{anom} is the corresponding anomaly and Nj is the total number of months j with available data.

It is well known that ground-based observations of cloudiness present certain limitations. On one hand, it is impossible to observe higher clouds concealed by lower ones. This is not an issue, however, when focusing our attention on TCC. In addition, there is the problem of observing clouds at nighttime (e.g., Hahn *et al.*, 1995). This should not significantly affect our results, as the same observation times (which include at least one night observation) were used for all stations and for the whole study period (see Section 2.1), and given that the analysis were performed with monthly data.

On the other hand, inherent uncertainty in the observation results from the subjectivity of the observer. Even if the observer is well trained and experienced, each particular observation presents a degree of uncertainty of around ±1 okta. Exceptions to this are the two extreme observations, that is, a totally cloudless sky (0 oktas) and a totally overcast sky (8 oktas). In these cases, the observation is easier, and the uncertainty is very much attenuated. This fact justifies the definition of the so-called "parameter of cloudiness" *PC* (Biel, 1963; Sanchez-Lorenzo *et al.*, 2012), which is computed in % according to the expression:

$$PC = 50 + 50\,\frac{Novcst - Nclear}{Ntot} \tag{2}$$

where *Novcst* and *Nclear* are the number of overcast and cloudless observations, respectively, in a given period, and *Ntot* is the total number of observations available for that period. Sanchez-Lorenzo *et al.* (2012) demonstrated the high correlation existing between the monthly mean TCC and *PC* anomalies. On the basis of this close correlation, *PC* was computed for each station as a way to further verify the quality of TCC observations: systematic biases may be detected on recording some particular cloudiness situations, because they will produce a lower correlation.

Specifically, we computed the monthly *PC* for each station and then the monthly *PC* anomalies (following the definition in Eq. 1), and analyzed the correlation with the monthly TCC anomalies. As stated above, the use of anomalies is justified because they avoid the high correlation already existent between the raw monthly series resulting from the seasonal cycle. In Figure 2 (left), the values for a particular station (Chimbaj, Uzbekistan) are plotted in order to show the typical close correlation existing between TCC and *PC* (r^2 = 0.98 for this particular site). In contrast, also in Fig. 2 (right) the plot for another site (Trabzon, Turkey) is presented: the behavior in this case is clearly different (r^2 = 0.69), so this is an example of a station that was not considered in the final database.

Following application of the above mentioned criteria, the database comprised a total of 185 stations. It is worth noting that for these remaining stations, most (97%) determination coefficients between the anomalies of *PC* and TCC are greater than 0.80, and many of them (69%) are greater than 0.90. The spatial distribution of these stations is presented in Fig. 1: in general terms they are evenly distributed in the area, although there is a higher density in the West and North of the Black Sea and a lack of stations in the East and South of the Caspian Sea. In particular, we were unable to maintain the stations in Georgia, Armenia, Azerbaijan, and Iran in the database, mainly because of long gaps in the data. Most series from the selected stations are complete and the data cover the whole time range; only 20 series (11% of 185) have over 10% (but less than 20%) of missing months. A table with the list of stations (including coordinates and country), is provided as Supplementary Material.

In addition to the analyses applied to each individual station, on one hand, and to the study domain as a whole on the other, we paid further attention to classifying stations according to their TCC temporal variability. We employed the Principal Component Analysis (PCA) technique to this end. We performed the analysis using the series of monthly-normalized anomalies (for mean to be equal to 0 and standard deviation equal to 1); each station is considered as a variable and each monthly anomaly, an observation. We used all months of the year in order to obtain only one classification result, thus avoiding finding different classifications for different temporal resolutions (Sanchez-Lorenzo *et al.*, 2007).

The results of the PCA showed that 17 Empirical Orthogonal Functions (EOF) account for more variance than each of the original variables (i.e., their eigenvalues are greater than 1) and explain over 86% of the total variance of the dataset. As a compromise between simplicity and explained variance, we selected the first eight EOF, which together explain over 78% of the variance (each of them explains over 3%). In order to redistribute the variance into the components and to obtain stable and physically meaningful patterns, we applied a Varimax rotation to the selected EOF (Von Storch, 1995). Subsequently, each station was assigned to one rotated component according to the maximum loading obtained from the PCA (Sanchez-Lorenzo *et al.*, 2007). This procedure sorted stations into eight relatively coherent (from the geographical and climatic points of view) regions. Figure 3 shows a graphical representation of the classes, which will hereinafter be referred to as regions. The assignation of a station to a region is detailed in the table in supplementary material. The regions and their acronyms used herein are NBS (North Black Sea), WBS (West Black Sea), SBS (South Black Sea), NC (North Caucasus), NCAS (North Caspian and Aral Seas), AAS (Around Aral Sea), SeAS (Southeast Aral Sea), SeCS (Southeast Caspian Sea). Despite these denominations, note that three stations in or next to the Crimea Peninsula belong to the SBS region, while one station on the eastern coast of the Caspian Sea is classified as an NC region.

We computed the annual, seasonal, and monthly mean series for each region and for the whole area by averaging all available data in each case. For the trend analyses, we computed the corresponding mean series of anomalies; in this case, missing data were filled with zeros. Using mean series provides a more synthetic description of the climatic signal than one single station and permits a higher signal-to-noise ratio, enabling better identification of long-term changes. The linear trends of the series were calculated by means of least squares linear fitting and their significance estimated by the Mann-Kendall nonparametric test (Sneyers, 1992).

For each of the additional datasets (Section 2.2) we first obtained the TCC monthly value for the grid cells within the area of interest. In addition to generating maps of mean TCC, we also computed the average series for the whole domain, as well as the average series of monthly and seasonal anomalies. As in the case of the observations, we used these to assess possible trends.

Finally, it should be noted that, since ground data ends in July 2010, and some gridded products end in 2009, all annual analyses were performed for the 1991-2009 period. On the contrary, where possible, seasonal analyses included January and February 2010, in order to use as many winters as other seasons.

4. Results and discussion

4.1. Climatology for the whole area on an annual and seasonal basis

Figure 4 shows the annual and seasonal mean TCC in the study area, for each station and for the 1991-2009 period. In addition, Table 1 shows the average values of TCC for the whole area both for the annual period and by seasons (winter: DJF; spring: MAM; summer: JJA; autumn: SON). The mean TCC for the area is 3.9 oktas (49 %TCC), but this value is produced by quite relevant spatial and seasonal variability.

Thus, annual TCC shows a remarkable latitudinal gradient, as well as a moderate longitudinal gradient. Sites with the lowest TCC (< 2.5 oktas) are located in the southeast of the area, specifically to the south of the Aral Sea. On the other side, stations with the highest TCC (> 5 oktas) are located in the northwest corner of the domain, although a second similar maximum is found to the north of the Caucasus, between the Black and the Caspian seas.

Figure 4 also shows that all seasons follow approximately the same pattern as the annual mean, but present clearly lower values in summer and higher ones in winter. Certain specific characteristics, however, can be derived from the seasonal maps. First, the spring maximum is located in the Caucasus region. Second, summer values are extremely low, especially in the south of the Black Sea and in the southeast of the area, where summer TCC is lower than 1 okta at several sites. Third, in winter there is a relatively high mean TCC (> 5.5 oktas) in regions such as between the Black and Caspian Sea and the north of the Black Sea.

Figure 5 gives the mean annual TCC as seen in the other datasets. It should be noted that in this figure the units are %TCC, but the transformation from oktas to %TCC is straightforward (1 okta = 12.5%TCC). The corresponding mean values for the whole area are given in Table 1. It is also noteworthy that the averages from the ground observations and from the gridded datasets are not strictly comparable, since the area covered by the latter datasets is somewhat larger and includes information referring to the sea; in addition, the average of the TCC from the ground stations was computed by assigning the same weight to all of them, despite their non-homogeneous distribution across the area. Moreover, the definitions of a cloud in terms of a satellite or of a reanalysis product may differ from the standard definition for a ground observer; the different temporal resolution of the original basic data may also affect the comparison.

The general spatial behavior (Fig. 5) is well captured by all datasets: in particular, they all show the latitudinal gradient, as well as the lowest values in the eastern part of the study area. Nonetheless, several particularities ought to be highlighted: the ISCCP mean annual TCC (53 %TCC) is slightly higher than that given by the ground stations (Table 1). CLARA exhibits the highest resolution of this dataset; this enables some local TCC maxima to be identified, such as in the southeast of the Black Sea, and in particular (perhaps erroneously) in the south of the Aral Sea. Mean annual TCC from PATMOS-x (48 %TCC) is very similar to that provided by the ground observations; indeed, the spatial pattern described by this product fits quite well with the ground observations. Values from the CRU dataset are virtually identical to the ground observations; this was to be expected, since the CRU dataset is built upon ground measurements, although it only uses daytime observations and a set of stations that is not necessarily the same.

The three reanalysis products clearly underestimate the annual mean TCC in the area. The range of values in the domain, from these three products, is 20-55 %TCC. Computed as the deviation for the whole area of the annual mean TCC, underestimations from the reanalyses are greater than -10 %TCC, reaching -15 %TCC for NCEP/DOE when compared with the ground observations (see Table 1). These values correspond to relative deviations (taking the ground observations as the reference) of over -20%. This remarkable underestimation has been previously reported for other areas (e.g., Weare *et al.*, 1995; Betts *et al.*, 2006; Bedacht *et al.*, 2007; Calbó and Sanchez-Lorenzo, 2009;Wu *et al.*, 2012; Naud *et al.*, 2014).

The values of mean annual TCC obtained from the ground observations (see Figure 4), as well as from most of the gridded products (Figure 5), are in agreement with global cloud climatologies (Warren et al., 1986; Warren and Hahn, 2002) and correspond to what is to be expected for such a mid-latitude area. For example, the values for winter plotted by Warren and Hahn (2002) in this area are approximately 40-70 %TCC, in full agreement with the values we found herein. Maximum cloudiness in the northwest is associated with low pressure systems travelling from the west at these latitudes, while the minimum in the south corresponds to the influence of the subtropical high pressure systems. Moreover, this minimum is enhanced in the eastern corner of the area because of the distance to any large water mass.

4.2. Variability and trends for the whole area

Figure 6 (top) shows the evolution of the monthly TCC mean for the whole area throughout the analyzed years for all data sources. All datasets suitably capture the amplitude of the annual cycle, with the maximum in winter and the minimum in summer. Relatively high values of TCC are often extended through the springtime, a pattern that is also captured by most products.

However, differences among the different datasets are also clear. For the ground observations, the winter maxima and the summer minima are approximately 5.5 and 2.5 oktas, respectively. Reanalysis products (in green in Figure 6, top) show the above mentioned large underestimation, with minimum values well below 2 oktas. Indeed, NCEP/DOE maxima never reach 4 oktas, so the large underestimation of TCC with NCEP/DOE data is mainly the result of underestimating the winter maximum. The three satellite-based products (shown in blue) very clearly follow the ground-based TCC evolution, especially during the final years of the series. These three products generally tend to produce a narrower yearly range, with lower maxima and higher minima. The PATMOS-x data are in slightly better agreement, whereas the minima provided by CLARA are always clearly higher than the ground observations. Among the gridded datasets, CRU (pink line) is the best one with regard to reproducing the variability of observations, confirming our findings in relation to the overall behavior presented in Section 4.1.

Figure 6 (bottom) shows the anomalies (of the mean TCC for the whole area) for all datasets. The relationship among them is now not so close: although the most important anomalies are captured by most datasets (see for example the strong anomalies in the second half of 1996, or in the 2008-2009 transition period), sometimes a particular anomaly is not produced by all of them, and even opposite-sign anomalies can be seen. Table 2 provides the correlations between the time series of monthly anomalies from each gridded dataset and the monthly anomalies from the ground observations. Strikingly, the highest correlations (0.58-0.64) correspond to the reanalysis products; this means that despite their systematic underestimation (see Section 4.1), the reanalyses quite correctly capture the temporal variability. Among the satellite products, the highest correlation is found for PATMOS-x (0.55), while CLARA reveals a very low correlation (0.41). The latter results tally with those of Sun et al. (2015) for the contiguous U.S. The correlation between anomalies from our ground-based observations and those from the CRU dataset is relatively low (0.49), considering that the latter was also developed on the basis of surface measurements. The CRU dataset, however, may be using different stations, and is built upon only diurnal observations; moreover, it sometimes makes use of proxy magnitudes (such as daily temperature range and sunshine duration) rather than direct observations of TCC (New et al., 2000; Harris et al., 2014).

Table 2 also shows the linear trends of the annual and seasonal TCC anomalies during the period analyzed, as derived from each dataset for the whole area. Based on the ground observations, the annual series show a statistically non-significant trend. The only slightly significant (90%) trend is found for the autumn data: +1.2 %TCC decade^{-1}. By contrast, most other datasets show significant negative trends, both for the annual series and also for most seasons, even in autumn. In this sense, the behavior of the CLARA dataset is clearly anomalous: all seasons show decreasing trends that are greater (in the absolute sense) than -4 %TCC decade^{-1} and the annual trend is -5.7 %TCC decade^{-1}. If this is certain, this would result in an 11 %TCC (almost 1 okta) reduction for the 19-year period. Since the average TCC in the area (according to the

CLARA data) is 53 %TCC, this would mean a relative TCC decrease of over 20%. The exaggeratedly large decreasing TCC trend shown by the CLARA dataset was also found in the U.S. by Sun *et al.* (2015). The other satellite products provide negative trends too, although much lower in absolute terms. The reanalysis datasets show a more moderate evolution, which are therefore more similar to the ground observations. Indeed, NCEP/DOE is the only dataset that does not produce any significant trend, so from this point of view, it is the one most parallel to the ground data. ERA and MERRA give negative trends, which are lower than those from the satellite products.

It should be noted that the 20–year period is somewhat short for a truly meaningful trend analysis. However, the results are in good agreement with other research dealing with the decadal variability of cloudiness in and around the area. In this sense, the statistically non-significant evolution of TCC observed in the study area is in line with the trends of ground-based records since the early 1990s over global land areas (Eastman and Warren, 2013). Likewise, the global time series of satellite-derived TCC do not show a clear trend over the last two decades (Palle and Laken, 2013; Stubenrauch *et al.*, 2012, 2013), or over the ocean during the last decade (March and, 2013). Indeed, stability in TCC since the 1990s is also observed in other regions of the World (Jovanovic *et al.*, 2011; Sanchez-Lorenzo *et al.*, 2012; Sanchez-Lorenzo and Wild, 2012; Free and Sun, 2014) despite the fact that sometimes a decrease (Sanchez-Lorenzo *et al.*, 2012; Eastman and Warren, 2013) or an increase (Free and Sun, 2014) has been described for previous years. For example, Eastman and Warren (2013) reported a statistically significant decrease of -0.4 %TCC decade^{-1} over global land areas from 1971 to 2009, but this was caused by high positive anomalies during the 1970s and early 1980s. It should be pointed out that, based upon the results of these authors

(Eastman and Warren, 2013), we can infer a mean decrease of -0.7 %TCC decade^{-1} for the study area and for the 1971-2009 period.

As previously mentioned, the TCC trends generated by other products show big discrepancies as compared with ground observations. It is worth noting that the study area is located at the edge of the geostationary satellite view. This is known to produce spurious negative trends in ISCCP records (Evan *et al.*, 2007; Norris, 2007; Norris and Slingo, 2009) that are no longer obvious when the artifacts have been removed from the data (Norris and Evan, 2015). Equally, other satellite-derived products such as CLARA and PATMOS-x have also been reported to show spurious negative trends during the last few decades, possibly due to an orbital drift in the sun-synchronous satellites used for the retrieval of their products (Norris and Slingo, 2009; Karlsson *et al.*, 2013). Thus, the results of the present study highlight the need to validate trends derived from satellite and reanalysis records of clouds by inter-comparing them (Stubenrauch *et al.*, 2013), and also by including traditional ground-based observations of clouds, which can help to distinguish between real climate variability and artifacts.

4.3. Climatology and trends on regional scale

Herein we describe the behavior of TCC in the eight regions defined by the PCA method (Section 3). We first computed the mean series of monthly TCC for each region by averaging the data from the corresponding stations. Moreover, we derived a mean annual cycle for each region by averaging the monthly data over all years. These mean annual cycles are displayed in Figure 7, while the annual and seasonal means for each region are given in Table 1. Two regions (NBS and NC) exhibit the highest TCC throughout the whole year, with a winter maximum of 6 oktas and a summer minimum greater than 3.5 oktas. Two other regions (WBS and NCAS) show a slightly lower summer minimum, while TCC is almost 1 okta lower in winter. The region with the lowest annual mean TCC (3 oktas), SeAS, has a summer minimum of approximately 1 okta (and < 1 okta in August), while the winter maximum is around 4.5 oktas. The other three regions (SBS, SeCS, AAS) lie somewhere in between. As a common feature for all regions, the summer minimum is reached in August, but it tends to be extended into September in the eastern regions (SeCS, SeAS, AAS, NCAS) and into July in the Western regions (NBS, WBS, SBS, NC). As for the winter maximum, values for December and January are very similar in all regions.

Subsequently, we computed and scrutinized the annual and seasonal anomalies to search for trends. Table 3 shows the results, which indicate that the averaging of anomalies for the whole area was hiding several regional trends of TCC. The most notable ones are found for the NC region: it presents a significant positive trend on an annual basis (+2.2 %TCC decade^{-1}), which is the result of large trends in autumn and winter (and also, but non-significantly, in spring). For some stations in this region, where cloud type data were available, we found that the increase in TCC is coupled with an increase in low cloud cover, which is also more marked in autumn and winter (not shown). Other neighboring regions (NCAS, WBS, NBS) also show positive (but non-significant) trends of TCC on an annual basis. In two of these latter regions (WBS, NBS) the annual positive trends result from large (and mostly significant) trends in autumn and winter. In the latter regions, however, non-significant trends in spring and summer are negative. In the region NCAS, the annual positive trend is mainly generated by the evolution of TCC in spring, which shows a significant trend. A similar positive trend in spring is found in the other north-eastern region (AAS).

On the other hand, the three southern regions behave quite differently. In SBS we found an annual negative trend (-2.2 %TCC decade^{-1}, significant) which results from negative trends in all seasons except autumn (although the winter trend is non-significant). The other two southern regions (SeAS, SeCS) do not reveal any significant trend, although the tendency indicates an increase in TCC in winter and spring and a decrease in summer and autumn.

Thus, the above results show that in spring there is a clear separation between the western regions (i.e., the three regions around the Black Sea), where TCC trends are negative, and the other regions, where trends are positive. On the contrary, in autumn and winter there are positive (and mostly significant) trends in the three northern regions around the Black Sea, whereas in the other regions trends are inexistent or slightly negative. In summer, there is no clear trend in any region, with the exception of one (SBS); however, the tendency, if any, is towards a decrease in TCC.

We also applied trend analysis per regions to the gridded products. That is, the values of TCC from the satellite, reanalyses, and CRU were averaged for the grid points approximately corresponding to the regions. Subsequently, anomalies were computed on an annual and seasonal basis, and trends were estimated. The results (not shown) are hardly compatible with what the ground observations indicated. For example, for region NC, where ground observations give mainly increasing TCC trends, all products (except CRU) generate negative trends. The exception is region SBS, where TCC trends are negative according to ground observations, and also according to most gridded products (although with different values and levels of significance). Surprisingly, the only product that produces contradictory trends for this region is CRU.

The trends found herein (or the lack of trends in some regions) can be compared with previous studies. For example, Eastman and Warren (2013) found clear reductions in the southwest regions (up to -1.8% decade^{-1}), which is in good agreement with our result for SBS, while they found smaller reductions, or even an increase (+0.3% decade^{-1}) in the northeast areas, i.e. in agreement with our non-significant trend in NCAS. It should be pointed out that a longer period (1971-2009) was studied by these authors. Chernokulsky *et al.* (2011) analyzed the same period as us (1991-2010), albeit only Russian stations, and found, as we did, an increase in TCC in the northeast of the Black Sea and the north of the Caucasus, particularly in autumn-winter. This is not surprising because the ground observations of cloudiness are likely the same or very similar.

Other studies in the area focus not only on cloudiness, but also on other variables that may be used as proxies. For example, Rahimzadeh *et al.* (2014) studied sunshine duration (SD) and diurnal temperature range (DTR) in Iran, as well as TCC. They found no DTR trends as from 1991 in northern Iran (and a slight non-significant decrease in TCC in summer), which is in line with the lack of significant trends that we found in the nearest region (SeCS). Furthermore, Yildirim *et al.* (2013) studied the behavior of SD in Turkey for the 1970-2010 period; specifically, and regarding the estimation of trends, they focused on two different subperiods, 1970-1990 and 1991-2010, the latter being coincident with our study period. They did not find any clear overall trend of SD for Turkey as a whole for the 1990-2010 period, but they found that several sites in the northern part of Turkey showed positive trends. This area coincides with region SBS, where we find a negative trend of TCC, which may partially explain the increase in SD. Even at seasonal resolution, the agreement is qualitatively good, since Yildirim *et al.* (2013) found significant positive trends at several stations in northern Turkey in spring and summer (thus corresponding with our negative trends of TCC in SBS for these two seasons).

Changes in TCC should be associated with changes in atmospheric circulation, provided that most cloudiness is of synoptic origin. Actually, this is not strictly so in the study area, where many clouds of mesoscale origin (i.e., convective clouds, orography-induced clouds, sea-breeze induced clouds) may exist, in particular in the warm part of the year. Nevertheless, some of the trends detected agree with changes in cyclonic activity in the area (Tilinina *et al.*, 2014), specifically a decrease in cyclones to the south of the Black Sea, especially in winter, and a moderate increase in cyclones to the north of the Black Sea, especially in summer. In general terms, these changes can be linked to the northward shift of the subtropical high pressure systems (Siedel *et al.*, 2008; Hu and Fu, 2007; Lu *et al.*, 2007).

In particular for the Aral Sea zone, cloud and precipitation are also modulated by invasion of cyclones from the south and south-west, wave activity, and western and north-western cold air intrusions. These types of synoptic activity along with topography and regional changes related to Aral Sea desiccation may be playing an important role in cloud variability in the AAS region. Due to the presence of a significant positive trend of TCC in spring in this Aral Sea region, we analyzed the time evolution of mean sea level pressure (MSLP) and precipitation fields as described by the NCEP/NCAR reanalysis. This revealed a tendency of MSLP to decrease in the region (up to -2.5 hPa decade^{-1}), while precipitation also showed an increase in spring for the last two decades (4 mm decade^{-1}). All these results agree well with each other: increased cloudiness and precipitation in spring are associated with intensification of activity of the South-Caspian, Murgab and Upper Amudariya cyclones, which is reflected in the pressure field configuration.

During the summer period, non-significant negative trends are revealed in the AAS, SeCS and SeAS regions. This fact is compatible with the statement by Chub (2003) that the proportion of summer and winter precipitation over the Aral Sea has changed. Prior to the desiccation period, the maximum of precipitation was in summer and this is now observed during the winter. Moreover, a significant decrease in relative humidity and an increase in DTR, especially in the south and east of the Aral Sea region, has been documented for summertime (Chub, 2003). The increase in DTR can be explained by the reduction of TCC, by means of modulation of radiative (both shortwave and longwave) fluxes.

5. Conclusions

The present study provides a description of the climatic behavior of total cloud cover (TCC) in the area of the three inland Eurasian seas (the Black, Caspian, and Aral seas). On the basis of data collected at almost 200 ground stations in the area, we found that average TCC is 3.9 oktas (49 %TCC). This figure, however, hides a large spatial and seasonal variability with minimum (maximum) TCC values in summer (winter) and in the southeast (northwest).

According to the temporal behavior of TCC, eight different regions are defined by means of a Principal Component Analysis. These eight regions share some common patterns, in particular a marked seasonal cycle, but also big differences as far as average TCC is concerned. Differences exceed 2.5 oktas (31 %TCC) in summer between the regions in the north of the Black Sea and the Caucasus mountains and the region located to the southeast of the Aral Sea.

Linear trend analyses of the ground-based observations of TCC have shown that for the whole area, TCC did not vary during the study period of almost 20 years (January 1991 – July 2010). Only in autumn, a weakly significant (90%) trend of +1.2 %TCC decade^{-1}

is detected over the whole domain. Again, the regional behavior is quite different. In the south of the Black Sea, clear decreasing trends are detected, both for the annual anomalies and also for spring and summer (values down to -4.3 %TCC decade^{-1}). In the north of the Caucasus, and the west and north of the Black Sea, increasing TCC is found for the annual series, mainly due to significant positive trends in autumn and winter (up to +5.0 %TCC decade^{-1}). In general, despite the relatively short period analyzed in the present research, all the findings regarding trends are in good correspondence with previous studies developed in different regions of the study area, either based on cloudiness data or based on proxy data such as sunshine duration or diurnal temperature range.

In addition to the ground observations, we also analyzed TCC data from a number of products offering gridded values. These products include satellite projects (ISCCP, PATMOS-x, CLARA), reanalyses (ERA-interim, NCEP/DOE, MERRA), and a dataset based on surface observations (CRU). Although all these products are able to capture the seasonal evolution over the study area, they differ substantially both among each other and in relation to the ground observations. Thus, for the whole area all reanalyses produce much lower values of TCC, while satellite data (ISCCP and CLARA) involve difficulties with regard to capturing the value of the summer minimum. Only CRU and, to a lesser extent, PATMOS-x data appear to agree quite well with the original surface observations referring to mean TCC, although monthly anomalies of all datasets correlate with the ground data anomalies (the highest correlations being found for the reanalyses). Global products should therefore be considered with caution when used to describe cloudiness, at least in this area. Moreover, this point is confirmed by the trend analyses applied to these data: most products generate negative trends, some of them being oddly large (CLARA gives a reduction of -5.7 %TCC decade^{-1}). The relative performance of PATMOS-x, ISCCP, and CLARA in their internanual variations and trends found in in this work is similar to that found by Sun et al. (2015), indicating that issues of the retrieval systems for those three satellite products are fundamental to the systems, independent of geographic regions. Only CRU and NCEP/DOE agree relatively well with the ground data regarding the absence of overall trends. It should be noted that direct comparison of these products with the ground-based data involves inherent limitations: first, because of the different points of view and even the different definition of what a cloud is; second, because of the different time sampling, which may hinder or enhance the description of the daily cycle; third, because each dataset has a different spatial resolution and representativeness.

In the future, there is a need to address two questions put forward by the current study. The first one entails establishing the causes and consequences of the trends in TCC that we have detected in some regions. That is, the decreasing cloudiness in some regions and the increase in other regions must be related either to changes in atmospheric circulation or atmospheric state (which could be linked to global climate change) or to variations in local conditions (land use/land cover, for example). In addition, these changes also have an impact at the local/regional scales, through modification of the energy balance. The second question refers to the reason why global gridded products, and in particular reanalyses, quite poorly reproduce ground observations of TCC. Despite the fact that several studies, applied to other regions, have already described this weakness, which may in part be related to the different definitions of clouds by different products, no conclusive results regarding their origin have been established. In this sense, continuity of ground-level observations is important with regard to detecting temporal changes. Finally, it is worth making a further effort to analyze cloud type behavior, i.e. temporal changes in low, middle, and high clouds, since this might be more informative of land-atmosphere interactions and could help to answer the other two questions.

Acknowledgements

This research was developed under the auspices of, and with funding from, the project "CLIMSEAS: Climate Change and Inland Seas: Phenomena, Feedbacks, and Uncertainties. The Physical Science Basis", of the Seventh Framework Programme, European Union People-Marie Curie Actions, International Research Staff Exchange Scheme (FP7-PEOPLE-2009-IRSES N. 247512). Several authors are involved within the project NUCLIERSOL (CGL2010-18546), funded by the Spanish Ministry of Economy and Competitiveness. Aarón Enriquez-Alonso was given a grant from the FPI program (BES-2011-049095) of the same ministry. Arturo Sanchez-Lorenzo was supported by the "Secretaria per a Universitats i Recerca del Departament d'Economia i Coneixement, de la Generalitat de Catalunya i del programa Cofund de les Accions Marie Curie del 7è Programa marc d'R+D de la Unió Europea" (2011 BP-B 00078) and the postdoctoral fellowship JCI-2012-12508. Partial support was provided to the Hydrometeorological Center of Russia by Russian Foundation for Basic Research (№13-05-00562). The ISCCP-D2 data were obtained from the International Satellite Cloud Climatology Project web site (http://isccp.giss.nasa.gov), maintained by the NASA Goddard Institute for Space Studies, New York. Data from EUMETSAT's Satellite Application Facility on Climate Monitoring (CM SAF) were used. PATMOS-x data are available via ftp from the University of Wisconsin, Space Science and Engineering Center (SSEC) and the Cooperative Institute for Meteorological Satellite Studies (CIMSS). ERA-Interim data are supported by the European Center for Medium-range Weather Forecast (ECMWF). NCEP Reanalysis data are provided by the

NOAA/OAR/ESRL PSD (http://www.esrl.noaa.gov/psd/). MERRA files were obtained from the NASA Goddard Earth Sciences Data and Information Services Center. CRU TS3.20 Time-Series (TS) of High Resolution Gridded Data were provided by the University of East Anglia Climatic Research Unit (CRU).

References

Arpe K, Leroy SAG, Lahijani H, Khan V. 2012. Impact of the European Russia drought in 2010 on the Caspian Sea level, *Hydrol. Earth Syst. Sci.*, 16: 19-27, doi: 10.5194/hess-16-19-2012.

Arpe K, Leroy SAG, Wetterhall F, Khan V, Hagemann S, Lahijani H. 2014. Prediction of the Caspian Sea Level using ECMWF seasonal forecasts and reanalysis, *Theor. Appl. Climatol.* 117(1): 41-60, doi: 10.1007/s00704-013-0937-6.

Aus der Beek T, Voßa F, Flörkea M. 2011. Modelling the impact of Global Change on the hydrological system of the Aral Sea basin, *Physics and Chemistry of the Earth, Parts A/B/C*, 36 (13): 684–695. doi: 10.1016/j.pce.2011.03.004

Bedacht E, Gulev SK, Macke A (2007) Intercomparison of global cloud cover fields over oceans from the VOS observations and NCEP/NCAR reanalysis. *Int. J. Climatol.* 27: 1707–1719. doi: 10.1002/joc.1490

Betts AK, Zhao M, Dirmeyer PA, Beljaars ACM. 2006. Comparison of ERA40 and NCEP/DOE near-surface data sets with other ISLSCP-II data sets. *J. Geophys. Res. Atmos.* 111. doi: 10.1029/2006JD007174

Biel, A. 1963. Nubosidad e insolación, Boletín Mensual Climatológico, Servicio Meteorológico Nacional, Madrid, 2–9. [in Spanish]

Boucher O, Randall D, Artaxo P, Bretherton C, Feingold G, Forster P, Kerminen VM, Kondo Y, Liao H, Lohmann U, Rasch P, Satheesh SK, Sherwood SW, Stevens B, Zhang XY.

2013. Clouds and Aerosols. In: Climate Change 2013: The Physical Science Basis. Contribution of Working Group I to the Fifth Assessment Report of the Intergovernmental Panel on Climate Change [Stocker, T.F., D. Qin, G.-K. Plattner, M. Tignor, S.K. Allen, J. Boschung, A. Nauels, Y. Xia, V. Bex and P.M. Midgley (eds.)]. Cambridge University Press, Cambridge, United Kingdom and New York, NY, USA.

Calbó J, Sanchez-Lorenzo A. 2009. Cloudiness climatology in the Iberian Peninsula from three global gridded datasets (ISCCP, CRU TS 2.1, ERA-40), *Theor. Appl. Climatol*. 96(1-2): 105–115, doi:10.1007/s00704-008-0039-z.

Cermak J, Wild M, Knutti R, Mishchenko MI, Heidinger AK. 2010. Consistency of global satellite-derived aerosol and cloud data sets with recent brightening observations, *Geophys. Res. Lett*. 37: L21704, doi:10.1029/2010GL044632.

Chernokulsky AV, Bulygina ON, Mokhov II. 2011. Recent variations of cloudiness over Russia from surface daytime observations, *Environ. Res. Lett.* 6: 035202. doi:10.1088/1748-9326/6/3/035202.

Chub, V. 2007 Climate Change and its Impact on Hydro-meteorological Processes, Agroclimatic and Water Resources of the Republic of Uzbekistan, Uzhydromet, Tashkent, Uzbekistan, 133p.

Costa-Surós M, Calbó J, González JA, Martin-Vide J. 2013. Behavior of cloud base height from ceilometer measurements, *Atmos. Res*. 127: 64–76, doi:10.1016/j.atmosres.2013.02.005.

Costa-Surós M, Calbó J, González JA, Long CN 2014. Comparing the cloud vertical structure derived from several methods based on radiosonde profiles and ground-based remote sensing measurements, *Atmos. Meas. Tech*., 7: 2757– 2773, doi:10.5194/amt-7-2757-2014.

Dai A, Karl T, Sun B, Trenberth K. 2006. Recent trends in cloudiness over the United States - A tale of monitoring inadequacies, *Bull. Am. Meteorol. Soc*. 87(5): 597–606, doi:10.1175/BAMS-87-5-597.

Dee DP, Uppala SM, Simmons AJ, *et al.* 2011. The ERA-Interim reanalysis: configuration and performance of the data assimilation system, *Q. J. R. Meteorol. Soc.* 137: 553–597. doi: 10.1002/qj.828.

Eastman R, Warren S G. 2013. A 39-Yr Survey of Cloud Changes from Land Stations Worldwide 1971–2009: Long-Term Trends, Relation to Aerosols, and Expansion of the Tropical Belt, *J. Clim*. 26: 1286–1303, doi:10.1175/JCLI-D-12-00280.1.

Evan AT, Heidinger AK, Vimont DJ. 2007. Arguments against a physical long-term trend in global ISCCP cloud amounts, *Geophys. Res. Lett*. 34: L04701, doi:10.1029/2006GL028083.

Flato G, Marotzke J, Abiodun B, Braconnot P, Chou SC, Collins W, Cox P, Driouech F, Emori S, Eyring V, Forest C, Gleckler P, Guilyardi E, Jakob C, Kattsov V, Reason C, Rummukainen M. 2013. Evaluation of Climate Models. In: Climate Change 2013: The Physical Science Basis. Contribution of Working Group I to the Fifth Assessment Report of the Intergovernmental Panel on Climate Change [Stocker, T.F., D. Qin, G.-K. Plattner, M. Tignor, S.K. Allen, J. Boschung, A. Nauels, Y. Xia, V. Bex and P.M. Midgley (eds.)]. Cambridge University Press, Cambridge, United Kingdom and New York, NY, USA.

Foster MJ, Heidinger A. 2013. PATMOS-x: Results from a Diurnally Corrected 30-yr Satellite Cloud Climatology. *J. Clim.* 26: 414–425. doi: 10.1175/JCLI-D-11-00666.1

Free M, Sun B. 2013. Time-Varying Biases in U.S. Total Cloud Cover Data. *J. Atmos. Oceanic Technol.* 30: 2838–2849.doi: http://dx.doi.org/10.1175/JTECH-D-13-00026.1

Free M, Sun B. 2014. Trends in U.S. Total Cloud Cover from a Homogeneity-Adjusted Dataset. *J. Clim.* 27: 4959–4969. doi: 10.1175/JCLI-D-13-00722.1.

Frolov AV. 2014. Second Assessment Report on Climate Change and its Consequences in Russian Federation, (Frolov A.V. ed) Roshydromet, Moscow, 61 p. [in Russian]

Gaybullaev B, Chen SC, Gaybullaev D. 2012. Changes in water volume of the Aral Sea after 1960, *Appl. Water Sci.* 2(4): 285-291.

Hahn CJ, Warren SG. 2003. Cloud Climatology for Land Stations Worldwide, 1971-1996. Numerical Data Package NDP-026D, Carbon Dioxide Information Analysis Center (CDIAC), Department of Energy, Oak Ridge, Tennessee (Documentation, 35 pages).

Hahn CJ, Warren SG, London J. 1995. The Effect of Moonlight on Observation of Cloud Cover at Night, and Application to Cloud Climatology. *J. Clim.* 8: 1429–1446.

Harris I, Jones PD, Osborn TJ, Lister DH. 2014. Updated high-resolution grids of monthly climatic observations - the CRU TS3.10 Dataset. *Int. J. Climatol.* 34: 623–642. doi: 10.1002/joc.3711.

Henderson-Sellers A. 1992. Continental cloudiness changes this century, *Geophys. J*. 27: 255–262.

Hu Y, Fu Q. 2007. Observed poleward expansion of the Hadley circulation since1979. *Atmos. Chem. Phys*. 7: 5229–5236.

IPCC, 2014: *Climate Change 2014: Impacts, Adaptation, and Vulnerability. Part B: Regional Aspects. Contribution of Working Group II to the Fifth Assessment Report of the Intergovernmental Panel on Climate Change* [Barros, V.R., C.B. Field, D.J. Dokken, M.D. Mastrandrea, K.J. Mach, T.E. Bilir, M. Chatterjee, K.L. Ebi, Y.O. Estrada, R.C. Genova, B. Girma, E.S. Kissel, A.N. Levy, S. MacCracken, P.R. Mastrandrea, and L.L. White (eds.)]. Cambridge University Press, Cambridge, United Kingdom and New York, NY, USA, 688 pp.

Jovanovic B, Collins D, Braganza K, Jakob D, Jones DA. 2011. A high-quality monthly total cloud amount dataset for Australia. *Clim. Change*, 108: 485-517.

L'Ecuyer T, Jiang J H. 2010.Touring the atmosphere aboard the A-Train, *Phys. Today* 63(7): 36–41.

Kaiser DP. 2000. Decreasing cloudiness over China: An updated analysis examining additional variables, *Geophys. Res. Lett*. 27(15): 2193–2196, doi:10.1029/2000GL011358.

Kanamitsu M, Ebisuzaki W, Woollen J, *et al.* 2002. NCEP–DOE AMIP-II Reanalysis (R-2). *Bull. Am. Meteorol. Soc.* 83: 1631–1643. doi: 10.1175/BAMS-83-11-1631.

Karlsson KG, Riihelä A, Müller R, *et al.* 2013. CLARA-A1: a cloud, albedo, and radiation dataset from 28 yr of global AVHRR data, *Atmos. Chem. Phys.* 13: 5351–5367. doi: 10.5194/acp-13-5351-2013.

Khan VM, Vil'fand RM, Zavialov PO. 2004. Long-term variability of air temperature in the Aral sea region, *J. Mar. Syst.* 47: 25-34.

Klebe DI, Blatherwick RD, Morris VR. 2014. Ground-based all-sky mid-infrared and visible imagery for purposes of characterizing cloud properties, *Atmos. Meas. Tech*. 7: 637–645, doi:10.5194/amt-7-637-2014.

Koronkevich N, Zaitseva I. 2003. Anthropogenic impacts on water resources. in Russia and neighboring countries at the end of XX century (Koronkevich N, Zaitseva I, Eds.). Nauka, Moscow. 367 p. [in Russian]

Long CN, Sabburg JM, Calbó J, Pagès D. 2006. Retrieving cloud characteristics from ground-based daytime color all-sky images, *J. Atmos. Ocean. Technol*. 23(5): 633–652, doi:10.1175/JTECH1875.1.

Lu J, Vecchi GA, Reichler T. 2007. Expansion of the Hadley cell under global warming. *Geophys. Res. Lett*. 34: L06805.

Marchand R. 2013. Trends in ISCCP, MISR, and MODIS cloud-top-height and optical-depth histograms, *J. Geophys. Res. Atmos*. 118, doi:10.1002/jgrd.50207.

Mescherskaya AV, Golod MP. 2003. About Long-range Forecasting of Caspian sea Level using Large-scale Climate Parameters, inHydrological and meteorological problems of the Caspian Sea and its drainage basin, St. Petersburg, pp 468–498 [in Russian].

Matuszko D, Weglarczyk S. 2014. Effect of cloudiness on long-term variability in airtemperature in Krakow, *Int. J. Climatol.* 34: 145 – 154, doi: 10.1002/joc.3672.

Nam C, Bony S, Dufresne JL, Chepfer H. 2012. The ‘too few, too bright’ tropical low-cloud problem in CMIP5 models. *Geophys. Res. Lett*. 39: L21801.

Naud CM, Booth JF. 2014. Evaluation of ERA-Interim and MERRA Cloudiness in the Southern Ocean. *J. Clim.* 27: 2109–2124.

New M, Hulme M, Jones P. 2000. Representing Twentieth-Century Space–Time Climate Variability. Part II: Development of 1901–96 Monthly Grids of Terrestrial Surface Climate. *J. Clim.* 13: 2217–2238.

Norris JR. 2005. Multidecadal changes in near-global cloud cover and estimated cloud cover radiative forcing, *J. Geophys. Res*. 110: D08206, doi:10.1029/2004JD005600.

Norris JR. 2008. Observed Interdecadal Changes in Cloudiness: Real or Spurious?, in *Climate Variability and Extremes during the Past 100 Years* (S. Brönnimann, J. Luterbacher, T. Ewen, H.F. Diaz, R.S. Stolarski, U. Neu, Eds.), Advances in Global Change Research, 33: 169-178.

Norris JR, Slingo A. 2009. Trends in Observed Cloudiness and Earth’ s Radiation Budget. What Do We Not Know and What Do We Need to Know? In *Clouds in the Perturbed Climate System: their relationship to Energy balance, Atmospherics Dynamics and Precipitation* (J Heintzenberg, RJ Charlson, Eds.). MIT Press.

Norris JR, Evan AT. 2015. Empirical Removal of Artifacts from the ISCCP and PATMOS-x Satellite Cloud Records, *J.Atmos. Ocean. Technol.*, doi: 10.1175/JTECH-D-14-00058.

Palle E, Laken BA. 2013. What do we really know about cloud changes over the past decades? *AIP Conf. Proc.* 1531, 66. doi: 10.1063/1.4804857.

Probst P, Rizzi R, Tosi E, Lucarini V, Maestri T. 2012. Total cloud cover from satellite observations and climate models, *Atmos. Res*. 107: 161–170, doi:10.1016/j.atmosres.2012.01.005.

Rahimzadeh F, Sanchez-Lorenzo A, Hamedi M, Kruk MC, Wild M. 2014. New evidence on the dimming/brightening phenomenon and decreasing diurnal temperature range in Iran (1961–2009), *Int. J. Climatol*. doi: 10.1002/joc.4107.

Ramanathan V, Cess RD, Harrison EF, Minnis P, Barkstrom BR, Ahmad E, Hartmann D.1989. Cloud-Radiative Forcing and Climate: Results from the Earth Radiation Budget Experiment, *Science*, 80, 243(4887): 57–63, doi:10.1126/science.243.4887.57.

Rienecker M, Suarez MJ, Gelaro R, *et al.* 2011. MERRA - NASA's Modern-Era Retrospective Analysis for Research and Applications, *J. Clim.* 24 (14): 3624–3648.

Roget E, Zavialov P, Khan V, Muñiz MA. 2009. Geodynamical processes in the channel connecting the two lobes of the Large Aral Sea, *Hydrol. Earth Syst. Sci*. 13, 2265–2271.

Rossow WB, Dueñas EN. 2004. The International Satellite Cloud Climatology Project (ISCCP) Web Site: An Online Resource for Research. *Bull. Am. Meteorol. Soc.* 85: 167–172. doi: 10.1175/BAMS-85-2-167

Rossow WB, Schiffer RA. 1999. Advances in Understanding Clouds from ISCCP. *Bull. Am. Meteorol. Soc.* 80: 2261–2287. doi: 10.1175/1520 -0477(1999)080<2261:AIUCFI>2.0.CO;2.

Rubinstein KG, Smirnova MM, Bychkova VI, Emelina SV, Ignatov RYu, Khan VM, Tischenko VA, Roget E. 2014. Investigation of Impact of Large Lakes Desiccation on Quality of Numerical Simulation of Meteorological Fields (Aral Sea Example), *Russian Meteorology and Hydrology* 11: 24-35.

Sanchez-Lorenzo A, Brunetti M, Calbó J, Martin-Vide J. 2007. Recent spatial and temporal variability and trends of sunshine duration over the Iberian Peninsula from a homogenized data set. *J. Geophys. Res*. 112: D20115, doi: 10.1029/2007JD008677.

Sanchez-Lorenzo A, Calbó J, Wild M. 2012. Increasing cloud cover in the 20th century: review and new findings in Spain, *Clim. Past* 8: 1199–1212, doi: 10.5194/cp-8-1199-2012.

Sanchez-Lorenzo A, Wild M. 2012. Decadal variations of estimated surface solar radiation over Switzerland since the late 19th century, 1885-2010, *Atmos. Chem. Phys*. 12: 8635–8644.

Seidel DJ, Fu Q, Randel WJ, Reichler T J. 2008. Widening of the tropical belt in a changing climate. *Nature Geosci*. 1: 21–24.

Shiklomanov I.A., A.S. Vasilieva, 2003. Hydrological and meteorological problems of the Caspian Sea and its drainage basin, St. Petersburg, 672 p. [in Russian]

Sneyers R. 1992. On the use of statistical analysis for the objective determination of climatic change, *Meteorol. Z.* 1: 247– 256.

Stevens B, Bony S. 2013. Water in the atmosphere, *Phys. Today*, 66: 29–34, doi:10.1063/PT.3.2009.

Stubenrauch CJ, Rossow WB, Kinne S. 2012. Assessment of global cloud datasets from satellites: A project of the World Climate Research Programme Global Energy and Water Cycle Experiment (GEWEX) Radiation Panel. WCRP Rep. 23/2012, 176 pp. [Available online at www.wcrp-climate.org/documents/GEWEX_Cloud_Assessment_2012.pdf.]

Stubenrauch CJ, *et al.* 2013. Assessment of global cloud datasets from satellite: Project and database initiated by the GEWEX radiation panel. *Bull. Am. Meteorol. Soc*. 94: 1031-1049.

Sun BM, Groisman PY. 2000. Cloudiness variations over the former Soviet Union, *Int. J. Climatol.* 20(10): 1097–1111, doi: 10.1002/1097-0088(200008)20:10<1097::AID-JOC541>3.0.CO;2-5.

Sun B, Free M, Yoo HL, Foster MJ, Heidinger A, Karlsson K-G. 2015. Variability and trends in U.S. cloud cover: ISCCP, PATMOS-x, and CLARA-A1 compared to homogeneity-adjusted weather observations, *J. Clim.* (in press) doi: http://dx.doi.org/10.1175/JCLI-D-14-00805.1

Tang Q, Leng Q. 2012. Damped summer warming accompanied with cloud cover increase over Eurasia from 1982 to 2009, *Environ. Res. Lett*. 7: 014004, doi:10.1088/1748-9326/7/1/014004.

Tilinina N, Gulev SK, Rudeva I, Koltermann P. 2013. Comparing Cyclone Life Cycle Characteristics and Their Interannual Variability in Different Reanalyses. *J. Clim.* 26: 6419–6438. doi: http://dx.doi.org/10.1175/JCLI-D-12-00777.1.

von Storch H. 1995. Spatial patterns: EOFs and CCA, in *Analysis of Climate Variability: Applications of Statistical Techniques,* (H. von Storch and A. Navarra, Eds.) pp. 227–258, Springer, New York.

Warren SG, Hahn CJ, London J, Chervin RM, Jenne RL. 1986. Global Distribution of Total Cloud Cover and Cloud Type Amounts over Land. NCAR Technical Note, NCAR/TN-273+STR, 29 pp. + 200 maps.

Warren SG, Hahn CJ. 2002. Cloud climatology. *Encyclopedia of Atmospheric Sciences* (J. R. Holton, J.A. Curry, J.A. Pyle, Eds.) Academic Press, London (UK), San Diego (CA, US), 476–483.

Warren SG, Eastman RM, Hahn CJ. 2007. A survey of changes in cloud cover and cloud types over land from surface observations, 1971-96, *J. Clim.* 20(4): 717–738, doi:10.1175/JCLI4031.1.

Weare BC, Mokhov II. 1995. Evaluation of total cloudiness and its variability in the atmospheric model intercomparison project. *J. Clim.* 8: 2224–2238.

WMO. 2012. Guide to Meteorological Instruments and Methods of Observation WMO-No. 8. World Meteorological Organization, Geneve, Switzerland, 716 pp.

Wu W, Liu Y, Betts AK. 2012. Observationally based evaluation of NWP reanalyses in modeling cloud properties over the Southern Great Plains. *J. Geophys. Res. Atmos.* 117. doi: 10.1029/2011JD016971.

Xia X. 2012. Significant decreasing cloud cover during 1954–2005 due to more clear-sky days and less overcast days in China and its relation to aerosol, *Ann. Geophys.* 30: 573-582, doi:10.5194/angeo-30-573-2012.

Yevteev O., Shatunova M., Perov V., Dmitrieva-Arrago L. 2010 The surface temperature variations due to the changes in solar flux and cloud water content (CWC), COSMO-RU simulation results. COSMO general meeting, Hydrometeorological Center of Russia, Moscow.

Yildirim U, Yilmaz IO, Akinoglu BG. 2013. Trend analysis of 41 years of sunshine duration data for Turkey, *Turkish J. Eng. Env. Sci.* 37: 286-305. doi:10.3906/muh-1301-11.

You Q, Jiao Y, Lin H, Min J, Kang S, Ren G, Meng X. 2014.Comparison of NCEP/NCAR and ERA-40 total cloud coverwith surface observations over the Tibetan Plateau, *Int. J. Climatol.* 34: 2529 – 2537, doi:10.1002/joc.3852.

Zavialov, P.O., Arashkevich, E.G., Bastida, I., *et al.* 2012. The large Aral Sea in the Beginning of the Century XXI. Physics, Biology, Chemestry. Nauka Publish., Moscow. 274 pp. [in Russian].

Table 1. Mean TCC for the 1991-2009 period (in %TCC) for the whole area and from the different datasets (rows 2 to 9). Idem for each of the regions defined by the PCA (see text), but only from the ground observations (rows 11 to 18). For the ground-based values, the corresponding amount in oktas is also provided (*in italics*).

Dataset	**Annual**	**Spring**	**Summer**	**Autumn**	**Winter**
Ground stations	49 (*3.9*)	53 (*4.2*)	34 (*2.7*)	47 (*3.8*)	65 (*5.2*)
ISCCP	53	59	40	49	62
PATMOS-x	48	55	33	43	62
CLARA	53	58	41	50	61
ERA-Interim	39	43	21	35	58
NCEP/DOE	35	38	24	32	44
MERRA	38	43	21	35	52
CRU	49	54	34	46	63
Regions					
NBS	60(*4.8*)	59(*4.7*)	45(*3.6*)	60(*4.8*)	75(*6.0*)
WBS	55(*4.4*)	58(*4.6*)	42(*3.4*)	55(*4.4*)	66(*5.3*)
SBS	45 *(3.6)*	50 *(4.0)*	25 *(2.0)*	42 *(3.4)*	62 *(5.0)*
NC	60(*4.8*)	62(*5.0*)	45(*3.6*)	58(*4.6*)	73(*5.8*)
NCAS	52(*4.2*)	52(*4.2*)	41(*3.3*)	50(*4.0*)	64(*5.1*)
AAS	41(*3.3*)	46(*3.7*)	26(*2.1*)	35(*2.8*)	57(*4.6*)
SeAS	38(*3.0*)	49(*3.9*)	16(*1.3*)	29(*2.3*)	58(*4.6*)
SeCS	40(*3.2*)	47(*3.8*)	22(*1.8*)	33(*2.6*)	55(*4.4*)

Table 2. Linear trends (in %TCC decade^{-1}) of the mean anomalies for the whole study area, on an annual and seasonal basis, during the 1991-2009 period. The second column is the regression coefficient between the series of monthly anomalies of each dataset and that derived from the ground observations.

Dataset	**R**	**Annual**	**Spring**	**Summer**	**Autumn**	**Winter**
Ground stations		n.t.	n.t.	–	1.2 #	+
ISCCP	0.47	-2.4 **	-3.1 *	-3.8 **	-2.7 *	n.t.
PATMOS-x	0.55	-2.2 **	-3.7 **	-1.6	-1.2	-2.3
CLARA	0.41	-5.7 **	-7.3 **	-5.0 **	-6.5 **	-4.1 **
ERA-Interim	0.64	-1.8 **	-3.1 *	-1.2 #	-1.4	-2.2 #
NCEP/DOE	0.60	n.t.	–	n.t.	n.t.	+
MERRA	0.58	-1.9 **	-3.5 **	-1.1	-1.9	-1.4
CRU	0.49	–	-1.1	-1.4	-1.0	1.2

Note: significance is indicated by # (90%), * (95%), and ** (99%). Other non-significant trends greater than 1 (in absolute value) are provided; lower trends are indicated only by their sign (+, increase; –, decrease). "n.t." means no trend at all (i.e. slope of regression line less than 0.05).

Table 3. Linear trends (in %TCC decade^{-1}) of the mean anomalies for the regions defined in the study area, on an annual and seasonal basis, during the 1991-2009 period.

Regions	**Annual**	**Spring**	**Summer**	**Autumn**	**Winter**
Wholearea	n.t.	n.t.	–	1.2 #	+
NBS	+	-2.6	–	2.9	3.5 #
WBS	1.1	-2.6	–	2.5 #	5.0 *
SBS	-2.2#	-4.3*	-3.0#	n.t.	-1.8
NC	2.2 *	1.8	n.t.	4.4 #	2.6 #
NCAS	1.3	3.7 #	n.t.	+	n.t.
AAS	n.t.	3.7 #	–	n.t.	–
SeAS	n.t.	+	-1.3	-	1.6
SeCS	n.t.	3.0	–	-1.2	n.t.

Note: significance is indicated by # (90%), and * (95%). Other non-significant trends greater than 1 (in absolute value) are provided; lower trends are indicated only by their sign. "n.t." means no trend at all (i.e. slope of regression line less than 0.05).

Figure captions

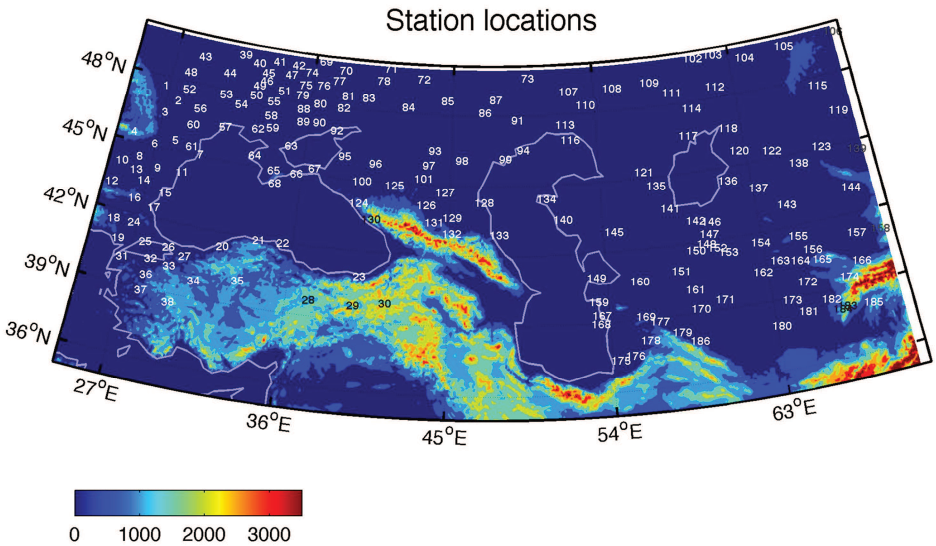

Figure 1. The study area, showing the contours of three inland seas, the main rivers, and the topography (color scale, in meters). Note that the profile of the Aral Sea corresponds to before-desiccation times. The location of the 185 stations with the cloudiness data considered is shown by means of an identification number as given in Table S1 (Supplementary Material).

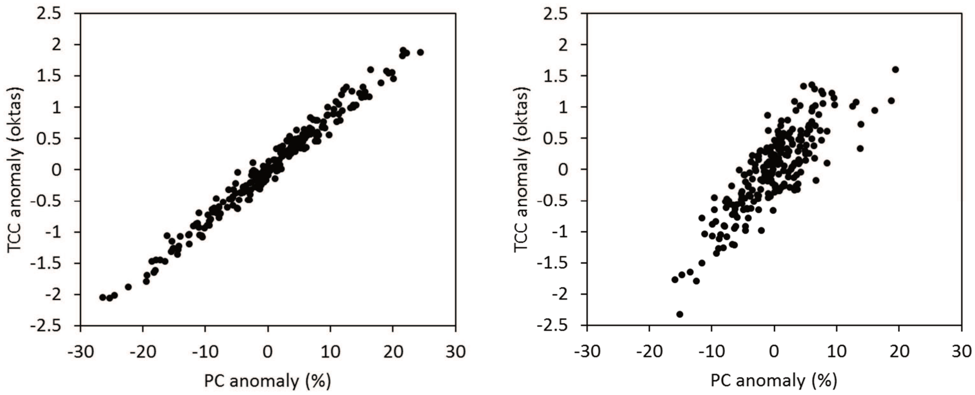

Figure 2. TCC anomaly vs. *PC* anomaly for the stations of Chimbaj, Uzbekistan (left) and Trabzon, Turkey (right).

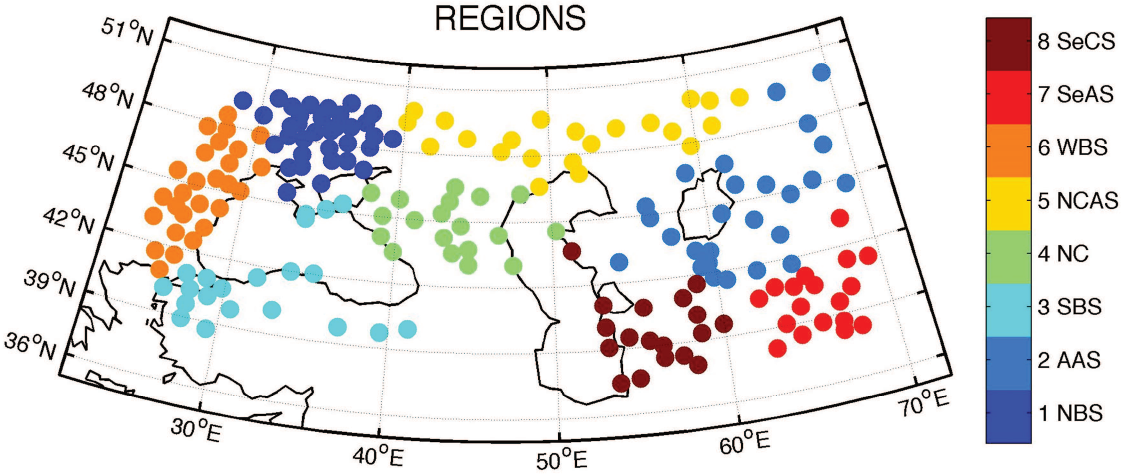

Figure 3. The study area, showing the classification of the stations into the eight regions defined by the Principal Components Analysis. Acronyms used for regions are as follows: NBS (North Black Sea), WBS (West Black Sea), SBS (South Black Sea), NC (North Caucasus), NCAS (North Caspian and Aral Seas), AAS (Around Aral Sea), SeAS (Southeast Aral Sea), SeCS (Southeast Caspian Sea).

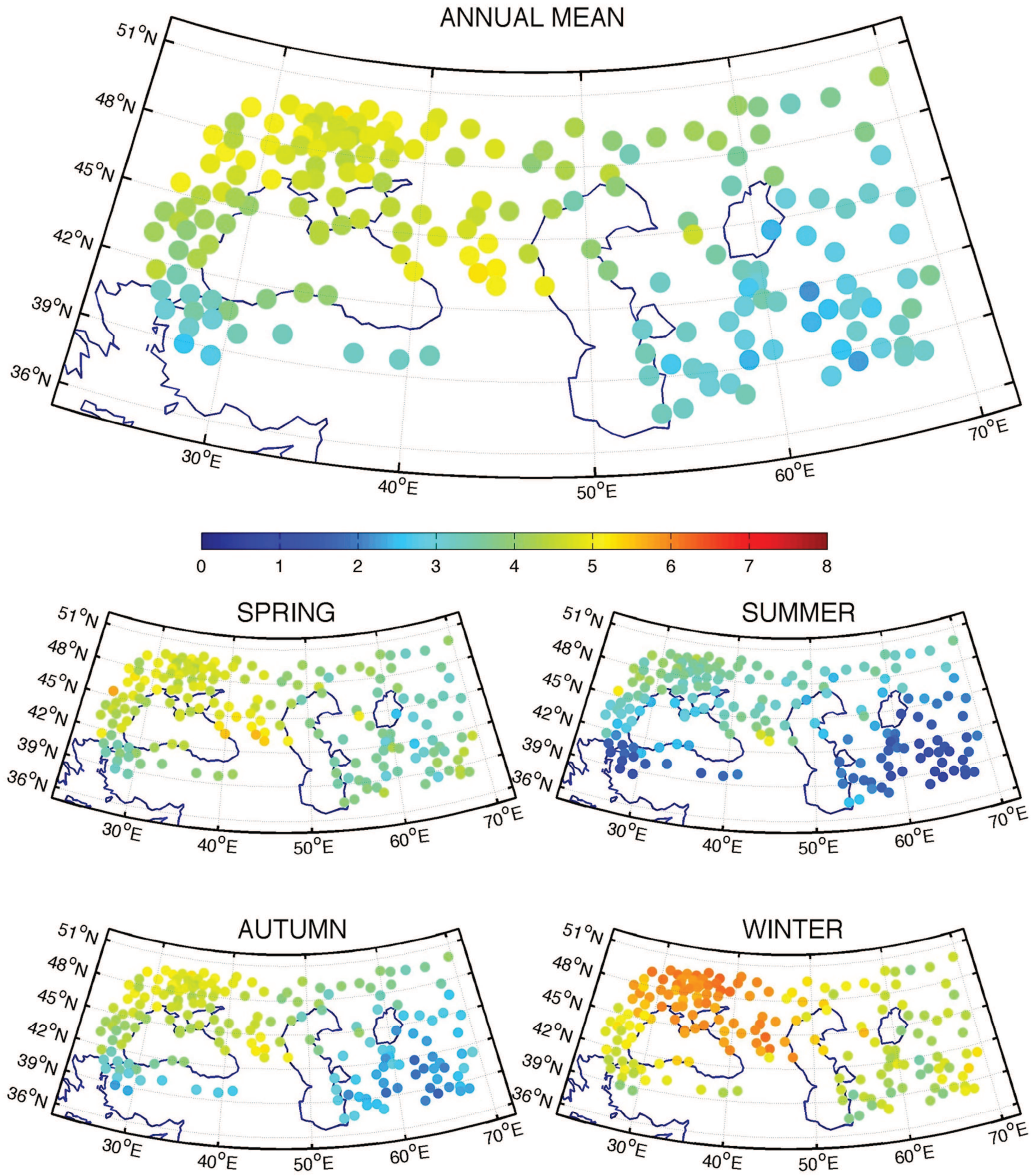

Figure 4. Mean TCC for the 1991-2009 period, for the whole year (top) and for each season (bottom). Units are oktas.

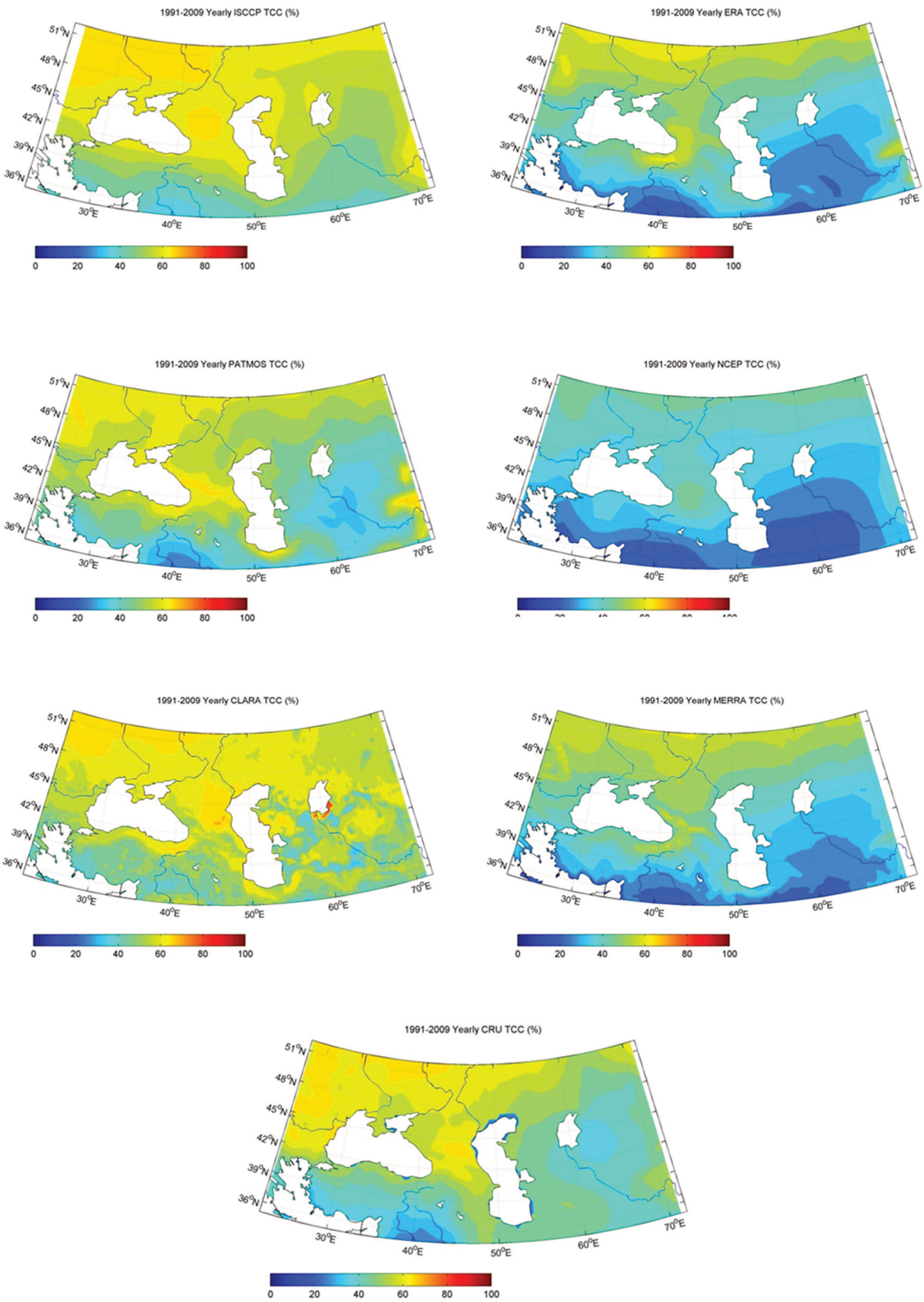

Figure 5. Mean annual TCC for the 1991-2009 period, as computed from different global gridded products, from satellite (left), reanalyses (right), surface data (bottom). Units are %TCC (1 okta = 12.5 %TCC).

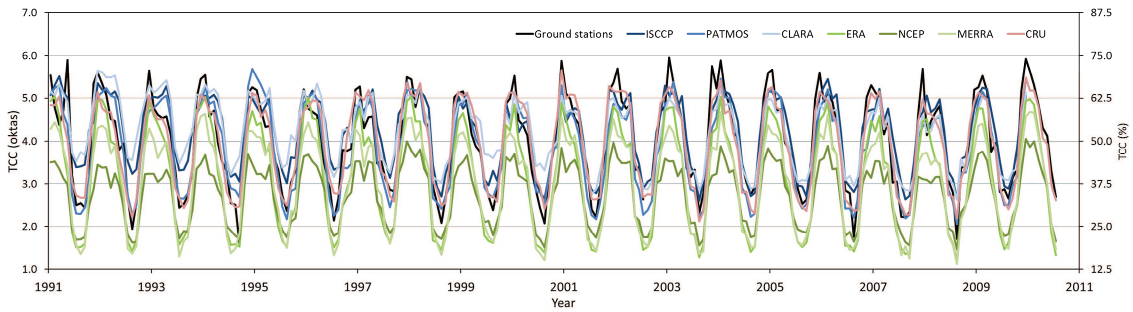

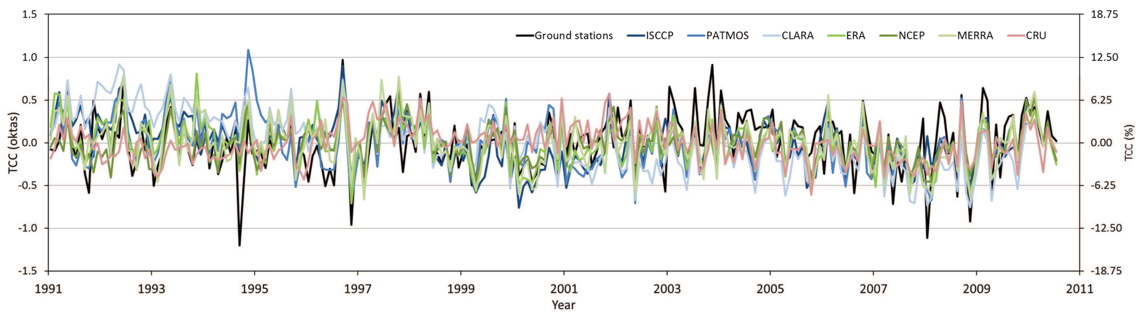

Figure 6. Evolution of the average monthly TCC for the whole area, as provided by each analyzed dataset (top). Evolution of the average monthly anomaly of TCC, as produced by each analyzed dataset (bottom).

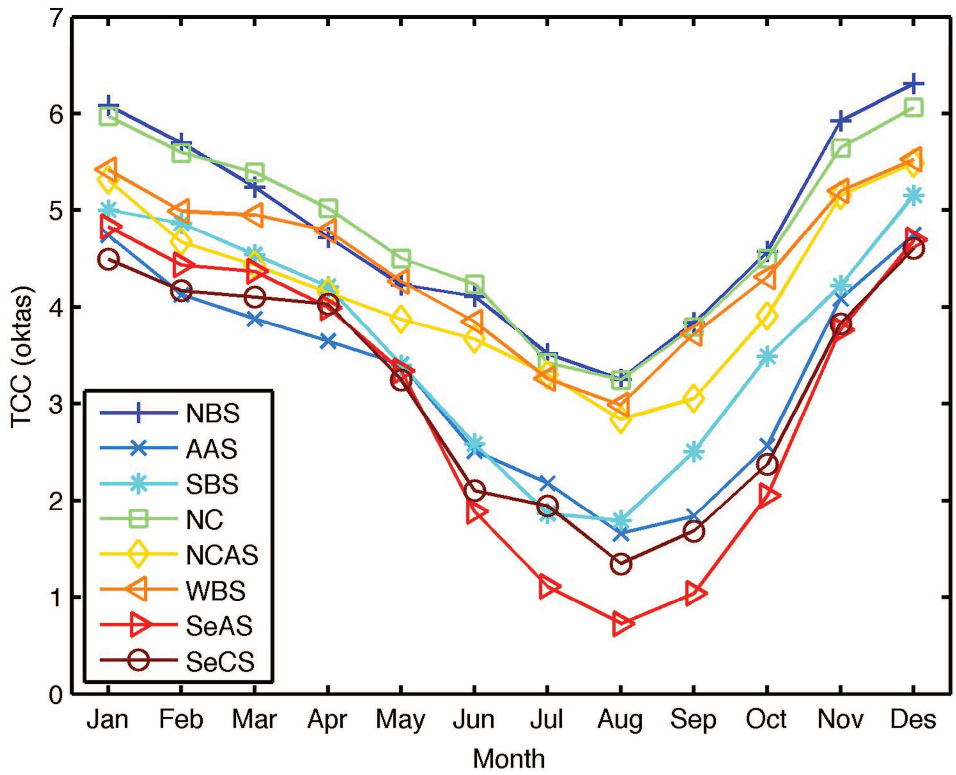

Figure 7. Mean annual cycle of TCC, i.e. monthly means for the 1991-2009/10 period, for each region defined by the PCA.